

Case Study of Wind-Induced Vibration of a Cooling Tower Under Typhoon Environment

XING Yuan¹, ZHAO Lin^{1,2*}, CHEN Xu¹, GE Yaojun^{1,2}

1. State Key Lab of Disaster Reduction in Civil Engineering, Tongji University, Shanghai 200092, P.R. China;
2. Key Laboratory of Transport Industry of Wind Resistant Technology for Bridge Structures, Tongji University, Shanghai 200092, P.R. China

(Received 27 October 2019; revised 9 January 2020; accepted 18 January 2020)

Abstract: As high-rise cooling towers are constantly emerging, wind effects on this kind of wind-sensitive structures have attracted more and more attention, especially in typhoon prone areas. Terrain Type B turbulent flow fields under the normal wind and typhoon are simulated by active wind tunnel technology, and rigid-pressure-measurement model and aero-elastic-vibration-measurement model of a large cooling tower are built. The stagnation point, peak suction point, separation point and leeward point of the throat position shell are selected to analyze pressure coefficient, probability distribution, peak factor, power spectral density and dynamic amplification factor under normal wind and typhoon. It is clarified that there exists a significant non-Gaussian characteristic under typhoon condition, which also exists in structural response level. Resonance response ratio of the total response is higher during typhoon condition. The maximum value of dynamic amplification coefficient under typhoon field is up to 1.18 times over that under normal wind. The findings of this study are expected to be of interest and practical use to professional and researchers involved in the wind-resistant designs of super-large cooling towers in typhoon prone regions.

Key words: cooling towers; active wind tunnel; non-Gaussian characteristic; wind-induced vibration; dynamic amplification coefficient

CLC number: TU33⁺2 **Document code:** A **Article ID:** 1005-1120(2020)01-0108-12

0 Introduction

The rapid development of economics, advances in construction materials and technologies continue to propel cooling towers to new heights and pose new design challenges for structural engineers. As an important part of the industrial cooling water cycle, cooling tower has been widely used, whose height has surpassed 200 m (in German, 2014) and 220 m (in China, 2019) in past decades. It is foreseeable that wind-resistant design of cooling tower as a large-span, high-rise, spatial, thin-walled structure is not an easy task since those structures are generally wind-sensitive due to the enhanced structural flexibility and stronger wind speed, particular-

ly in typhoon prone regions. It is well known that strong typhoons, a rapidly rotating storm system with a low-pressure center, belong to most destructive natural disasters in the world.

Wind loads on large cooling towers are often considered as the predominant load among all potential loading combinations, such as weight, temperature, seismic action, uneven settlement, etc., during the whole life cycle^[1]. In 1965, three cooling towers in the leeward region of a rhombic arrangement with eight-tower two-column type collapsed under only a moderate wind speed with five-year return period in Ferrybridge Power Plant, UK and significant vibration phenomenon was reported^[2]. Since then, in-situ measurements and wind tunnel tests were

*Corresponding author, E-mail address: zhaolin@tongji.edu.cn.

How to cite this article: XING Yuan, ZHAO Lin, CHEN Xu, et al. Case study of wind-induced vibration of a cooling tower under typhoon environment[J]. Transactions of Nanjing University of Aeronautics and Astronautics, 2020, 37(1): 108-119.

<http://dx.doi.org/10.16356/j.1005-1120.2020.01.010>

performed to research wind pressure characteristics over the surface of cooling towers^[3-9]. Investigations focusing on wind-induced stochastic dynamic response for shell structures^[10-16] were also conducted.

It is well known that wind characteristics of typhoon climate reported by ever-increasing amounts of observation data were obviously different from wind characteristic of normal wind, increasing boundary layer height^[17-18] and enhancing turbulence gust factor value and turbulence intensity^[19-20]. Zhao et al.^[8] found turbulence intensity had an significant impact on fluctuation wind pressure of cooling towers. Based on in-site measurement for super-tall buildings, Zhang et al.^[21] reported significant non-Gaussian characteristic under typhoon environment. Ke et al.^[15] found that the non-stationary model can better characterize the measured wind-induced responses of a super-large cooling tower. Based on the early cooling tower elastic model wind tunnel test, the dynamic stress and static stress of the cooling tower under the wind load had the same magnitude, and the resonance effect increased according to the fourth power of the wind speed, which was much higher than the quasi-static stress growth rate^[1]. Winney^[10] reported the notable resonance effect through field measurement. Furthermore, Jeary et al.^[22] measured the 126.31 m high cooling tower in a typhoon environment with a resonance response at a maximum gust condition of 6 m/s. The influence mechanism of the typhoon climatic on structural response is complicated due to its special characteristics. So, it is necessary to further systematically study the wind pressure characteristic and structural response of cooling towers under typhoon as a structural design reference. Compared with in-sit measurement, wind tunnel test is a feasible way to research typhoon-induced adverse effect with the development of active wind tunnel test technology^[23-25].

1 Overview of Wind Tunnel Tests

1.1 Wind field simulation

A large cooling tower located on the coast line of China is chosen as a case study and the wind field

of a terrain Type B turbulent flow field was chosen as simulation target. Generally, the vertical variation of mean wind speed, which is mainly controlled by the evolution of upstream surface roughness, is considered to follow a power law (Eq. (1)) for strong winds in a neutrally-stable atmospheric boundary layer adapted into wind design guidance by most countries^[26]. In order to attain mean wind profile index α , a large number of direct observations of typhoon vertical profiles had been conducted and Monte-Carlo numerical simulation was performed. More attention is paid on structural wind loads and response in this paper. So, the simulation results are shown directly.

$$U(z) = U(10) \cdot \left(\frac{z}{10} \right)^\alpha \quad (1)$$

where $U(z)$ represents wind speed at z height, $U(10)$ the 10 m-height design wind speed, and α the mean wind profile index, which is 0.097 for typhoon and 0.15 for normal wind^[27], respectively.

The fluctuating characteristics of wind employed in engineering applications are usually quantitatively represented by power spectrum density (PSD), turbulence intensity and turbulence integral scale. The turbulence spectrum was proved to follow the von Kármán model (Eq. (2)) in longitudinal direction by Cao et al.^[25], Masters et al.^[28] and Balderrama et al.^[29].

$$S_u(f) = \frac{4 \cdot I_{uT}^2 \cdot L_u^x \cdot U}{\left(1 + 70.8 \frac{f \cdot L_u^x}{U} \right)^{\frac{5}{6}}} \quad (2)$$

where S_u is the Von Karman spectrum function, f the frequency, U the wind speed, I_{uT} the turbulence intensity, and L_u^x the turbulence integral scale of the along-wind direction. As compared by Kwon et al.^[30], in most codes or standards, turbulence intensity profile is also expressed in terms of a power law as

$$I_{uT}(z) = c_T I_u(z) = c_T I_{u10} \left(\frac{z}{10} \right)^\alpha \quad (3)$$

where $I_{uT}(z)$ and $I_u(z)$ represent the turbulence intensity in typhoon and normal wind, and c_T is 1.48 for terrain Type B suggested by Sharma and Richards^[20]. Correspondingly, $I_{u10} = 0.14$ as recommended by the China national code^[27].

Turbulence integral scale is a measure of the size of energy-containing eddies that corresponds to the largest magnitude of the turbulence PSD. Because the PSD of strong typhoon winds is consistent with the commonly-used von Kármán model, it is reasonable to assume that the longitudinal turbulence integral length scale can be described by the code specifications. In this study, turbulence integral scale is chosen from the AIJ Code, Japan^[31] (Eq.(4)), shown as

$$L_u^x = \begin{cases} 100 & z \leq 30 \text{ m} \\ 100 \times \left(\frac{z}{30}\right)^{0.5} & 30 \text{ m} < z < H_G \end{cases} \quad (4)$$

where L_u^x is the turbulence integral scale and H_G the gradient wind height, which is 1 400 m for typhoon and 350 m for normal wind^[27], respectively.

Synchronous pressure measurement tests were undertaken in 3-D multi-fan active control wind tunnel (Fig.1) consisting of 99 independent fans in Miyazaki University, Japan. This wind tunnel is an open-circuit one with 99 fans of 270 mm in diameter at the front. The fans are arranged in a 9 wide by 11 high matrix. The test section is 15.5 m length, 2.6 m width, and 1.8 m height. The spatial distributions of some turbulent parameters, such as mean velocity, turbulent intensity, integral scale, power spectrum and Reynolds stress, etc. have been successfully reproduced in the wind tunnel^[23-24,32-33]. In order to attain simulated wind field characteristic of the Type B ABL turbulent flow field, Cobra probes placed on a height-moveable bracket (Fig.2) were chosen to measure wind velocity time history which was sampled every 5 cm-height interval (about 30 m height corresponding to prototype) with 1 000 Hz sampling frequency.

The simulation results of mean wind speed, turbulence intensity and turbulence integral scale shown in Fig.3 and Fig.4 were closed to targets suc-

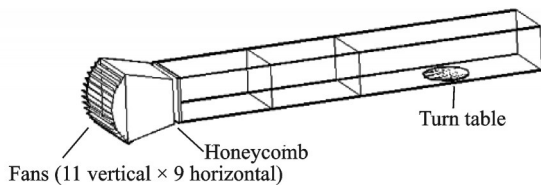


Fig.1 Schematic of the 3-D multiple-fan wind tunnel

cessfully. Comparing Fig. 3 (a) with Fig. 4 (a), stronger turbulence intensity and larger turbulence

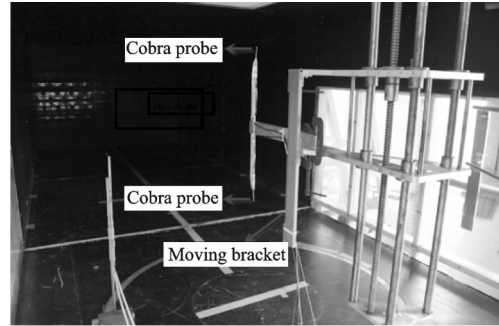
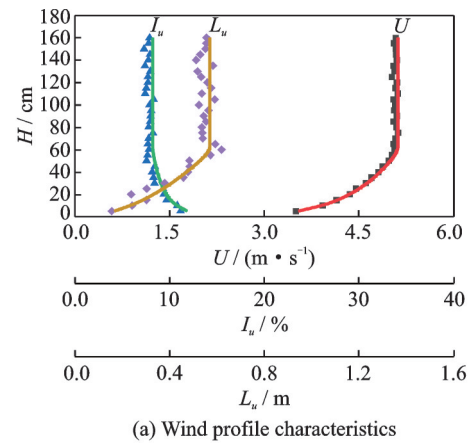
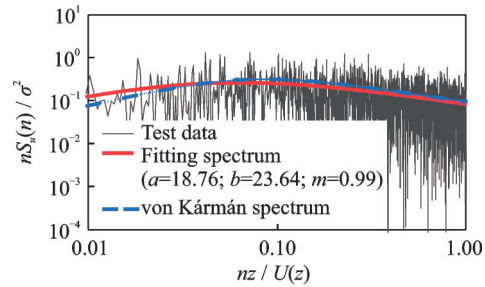


Fig.2 Cobra probe placement during wind field measurement

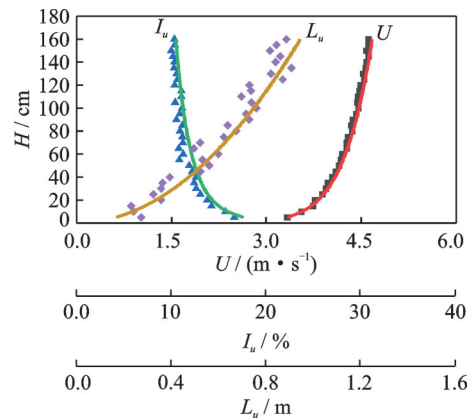


(a) Wind profile characteristics



(b) Power spectral density of downwind

Fig.3 Turbulence characteristics for a terrain Type B flow field under normal wind



(a) Wind profile characteristics

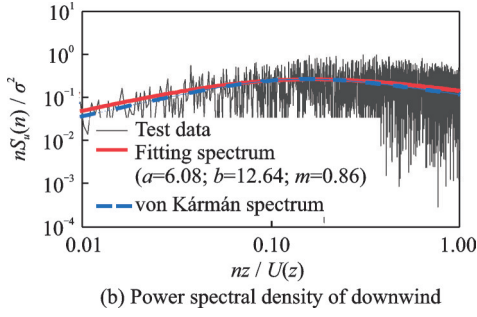


Fig.4 Turbulence characteristics for a terrain Type B flow field simulated under typhoon

integral scale were formed in typhoon field up to 1.7 and 1.1 times than those in normal wind field at 36 cm height (the top of the cooling tower). What's more, the renormalized fluctuation wind speed spectrums of the downwind direction at 36 cm height during the typhoon approximately follows the von Kármán spectrum consistency with references by Tamura et al.^[34] and Cao et al.^[25], which were fitted by Eq.(5). It is clear from Fig.3(b) and Fig.4 (b) that the turbulence spectrum is lower from 0.01 Hz to 0.1 Hz and higher from 0.1 Hz to 1 Hz under typhoon.

$$nS_u(n)/\sigma^2 = af_z^r / (1 + bf_z^{1/m})^{cm} \quad (5)$$

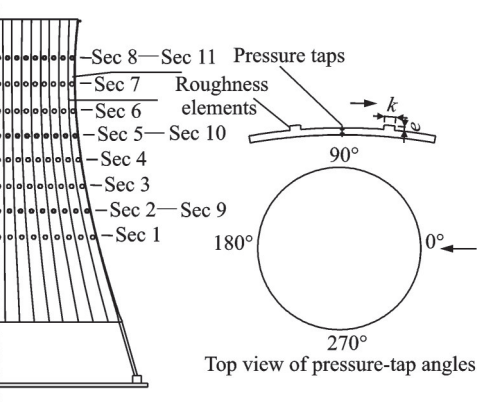
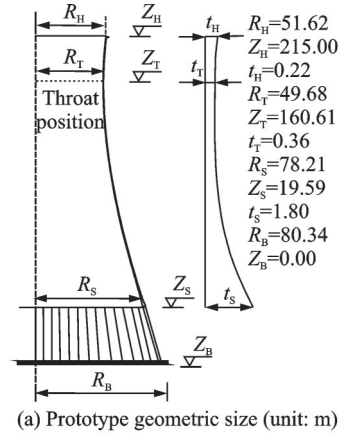
where a , b , c , m are fitting coefficients. According to turbulent energy spectrum theory proposed by Kolmogoroff^[35], c and r obey Eq.(6), furthermore, r is 1 and c is 5/3 in general; n is the frequency and σ the sampling time variance. And f_z is reduced frequency following Eq.(7).

$$c - r = 2/3 \quad (6)$$

$$f_z = nz/U(z) \quad (7)$$

1.2 Test models

A 1: 600 scaled rigid pressure measurement model and aero-elastic model were produced based on 215 m high cooling tower, which were used to record external wind pressure measurements and attain structural dynamic response. The shape of the cooling tower is shown in Fig.5(a), whose height is 215 m and in which Z , R and t represent height, radius and thickness, subscripts H, T, S and B represent top, throat, inlet and bottom of the tower shell. The rigid model was designed with 36×8 external pressure measurement taps uniformly distributed along the circumferential and meridian directions, re-



(b) Distribution of pressure measurement points on the rigid models
Fig.5 Geometric dimensions and layout of pressure taps on the cooling tower model

spectively. The distribution of the taps (and number) around the circumferential section is shown in Fig.5(b), where Sec represents the measured section, and e , k represent height and width of roughness elements, respectively. Wind pressure was measured using a DSM3000 electronic pressure scanning valve (Scanivalve Company) with a sampling frequency of 500 Hz. A total of 30 000-point data were produced at one measurement point during each run. The Reynolds number (Re) regime for flow around the prototype large cooling towers was $1.5 \times 10^8 - 3.5 \times 10^8$ based on the design wind speed. Due to size limitations of the test model, realistic wind effects for a high Re cannot be easily reproduced by increasing the test wind speed and the model size. However, wind flow around a cylinder does not only depend on the Re number, it is also closely related to the surface roughness of the cylinder. Previous investigations^[36-37] have shown that wind effects on a cylinder with a high Re number effect can be reproduced on a scale model by increasing the sur-

face roughness of the model. After comparing several types of surface roughness, attaching 36 uniformly distributed four-layered vertical paper tapes (Fig.5 (b)) with a specific test wind speed was identified to be the optimal approach to compensate the effects of a post critical Re number. The simulation criteria involve the mean and fluctuation wind pressure distributions (Fig.6). In Fig.6, RE is the roughness element height.

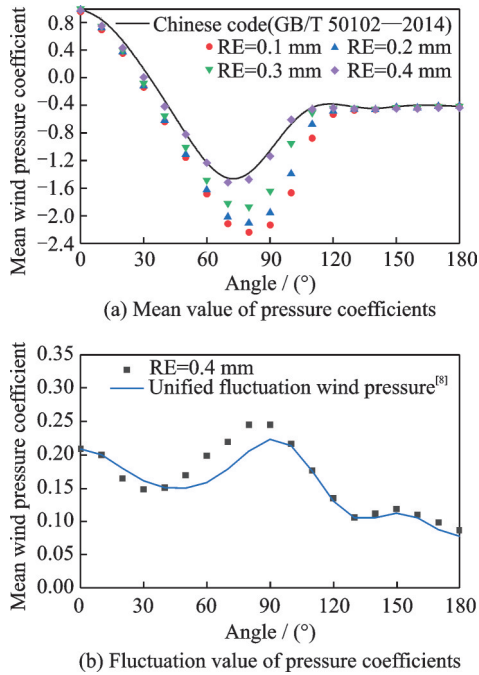


Fig.6 Reynolds number effects simulation of experimental model

The aero-elastic models of large cooling towers were tested in the wind tunnel by Armitt^[1], Isyomov et al.^[38] and Zhao et al.^[39] in previous studies. Design methods of the aero-elastic model mainly consist of the continuous medium method and the equivalent beam-net method. Our previous research indicated that the former was suitable for destructive tests of cooling towers, and the latter could be used to study on wind-induced responses of cooling towers^[12,39]. In this study, we mainly focus on the structural vibration response induced by various wind field, so the aero-elastic model is designed through an equivalent beam-net method. Limited to research subject of this article, the detailed design and produce process of aero-elastic model can be found in Ref.[39]. The aero-elastic model is shown in Fig.7

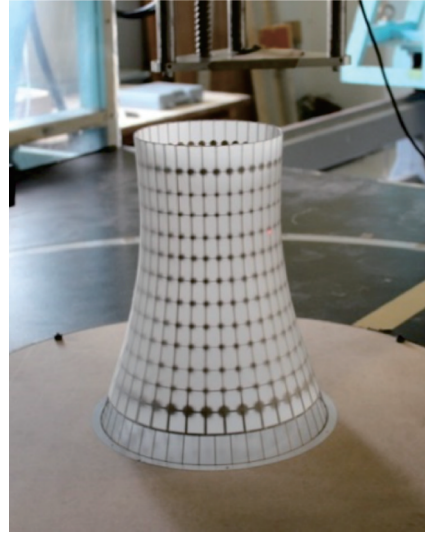


Fig.7 Aero-elastic model for simultaneous pressure and vibration measurement

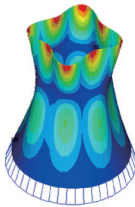
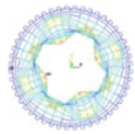
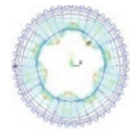
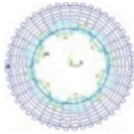
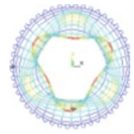
and dynamic characteristics of the aero-elastic model are shown in Table 1.

Model shapes of front four orders were attained from aero-elastic model are consistence with prototype structure's model acquired by FEM calculation. The design deviation of the first mode is 1.12% and the damping ratio of the first-order mode is 3.1%, which satisfies the empirical damping ratio requirement of the concrete structure^[27]. Reynolds number effects simulation was also performed. The simulation method is introduced in Section 1.1 in detailed.

2 Wind Pressure Characteristics for a Cooling Tower

Throat region is the adverse position in structural analysis^[13], so wind pressure coefficients and structural response of throat position shells are paid more attention in the following analysis. It is clear from Fig.8(a) that fluctuation wind pressure coefficients under Typhoon are significantly higher than those of normal wind, because stronger turbulence intensity and larger turbulence integral scale, up to 1.5 and 1.2 times separately. Sadeh et al.^[40] thought turbulence vortex of free-stream turbulence attain energy from some particular signature scale turbulence vortex, which was called vortex amplification

Table 1 Mode shapes and dynamic characteristics of the design model and prototype structure

Mode		1	2	3	4
Prototype structure	Shape profile				
	Frequency / Hz	0.84	0.88	0.99	1.01
Aero-elastic model	Shape profile				
	Test frequency/ Hz	20.43	21.70	24.64	25.19
	Design frequency & frequency error / %	(20.21, 1.12)	(21.14, 2.67)	(23.95, 2.80)	(24.57, 2.46)
	Circumference & Meridian harmonic number	4 & 2	5 & 2	6 & 2	3 & 1

theory. Based on filed measurement and wind tunnel test, Zhao et al.^[8] found that fluctuation wind pressure is positively correlated with turbulence intensity further, thus illustrating this amplification effect.

Fig.8 (b) shows peak factors calculated by Sadek-Simiu method^[41] which is suitable to non-Gaussian wind pressure samples^[9,21]. Peak factors are bigger from 0° to 60° zone, while appearing opposite phenomenon from 75° to 135° region. There is no obvious relationship between the magnitude of turbulence intensity and the peak factor, which was also reported by Cheng et al.^[9].

It is well-known that aerodynamics assumes wind pressure generated by countless different scale point vortices whose energy obeys stochastic process that is Gaussian process. When organized vortices are of larger ratio among the various turbulence components, non-Gaussian phenomenon appears. To further analyze mechanism, it is necessary to research non-Gaussian phenomenon. Fig.9 shows probability and statistical characteristics of wind pressure coefficients of four key points including the stagnation point (0°), the peak suction point (70°), the separation point (120°) and the leeward point (180°). No matter which kind of wind field is in the test, wind pressure coefficients of the stagnation point and the leeward point are

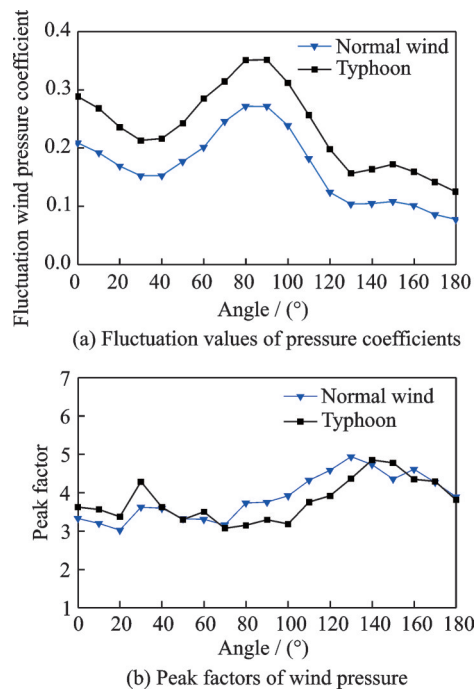


Fig.8 Root variances and peak factors of wind pressure under normal wind and typhoon

close to Gaussian distribution. However, significant skewness and kurtosis appear in the separation point caused by separation vortex and it is crucial that typhoon obviously emphasize this phenomenon. Fig.10 shows renormalized power spectrum of peak suction point and separation point. there is a peak value around 5 Hz (separation vortex frequency) and the peak value is higher during typhoon, because free-stream turbulence affects the vortex

energy component of signature turbulence resulting in more organized vortex formation. Typhoon gives

rise to significant amplification effect on wind pressure load.

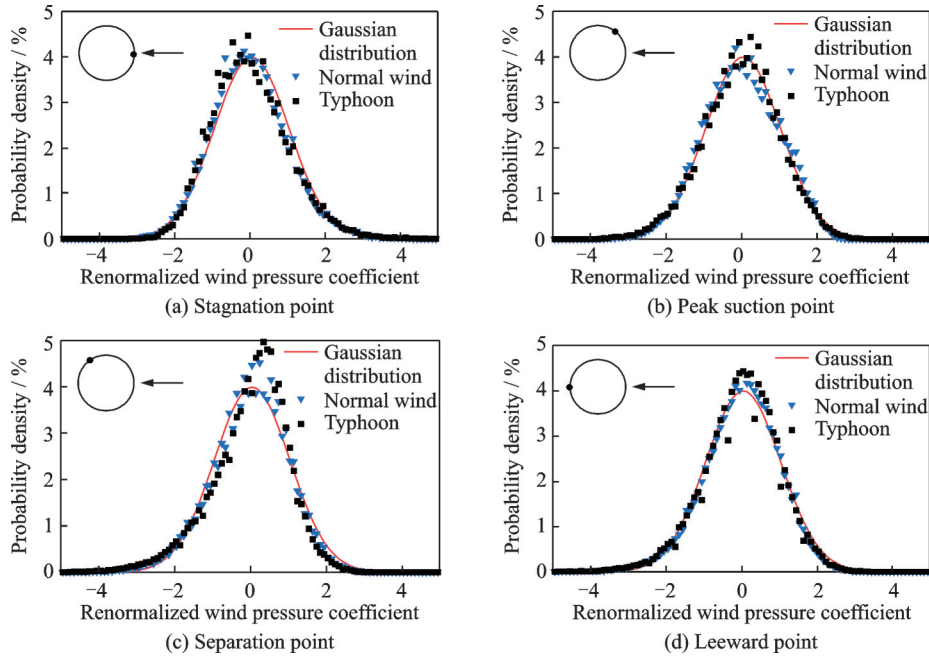


Fig.9 Probability density distribution of four throat-region points under normal wind and typhoon

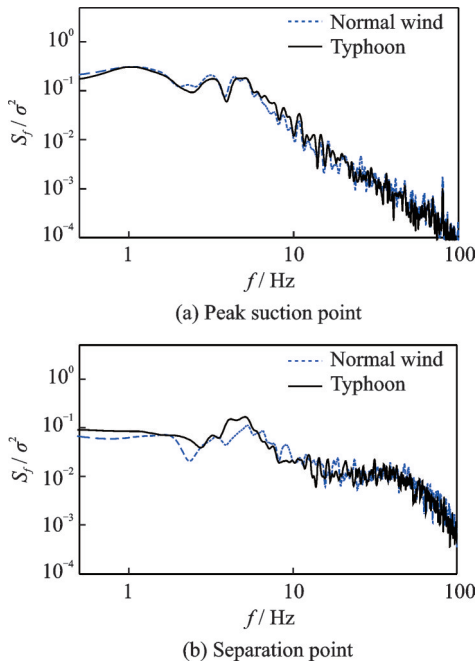


Fig.10 Renormalized wind pressure spectrum in normal wind and typhoon

3 Wind-Induced Performance

3.1 Structural response analysis

Fig.11 shows the renormalized structural displacement response spectrum of four points on the

cooling tower shell at throat position. Stochastic fluctuation wind pressure leads to multi-order resonance modes excited, which is consistency with relevant research work based on field measurement and FEM calculation^[10,12]. The resonance responses of the first, second and fifth modes are more appearance at typhoon condition, while the resonance responses of the third and eighth modes are less. Fig.12 is background and resonance response ratio of total response under typhoon and normal wind. The resonance response ratio of total response of the stagnation point is the highest. The resonance response ratios of all points are amplified under typhoon condition. it is can be considered that wind pressure distribution formed by more organized vortex in typhoon field is easier to excite resonance response.

Peak factors are similar in structural response level (Fig.13). Probability density distributions of structural displacement response of three throat-region points (Fig.14) under normal wind and ty-

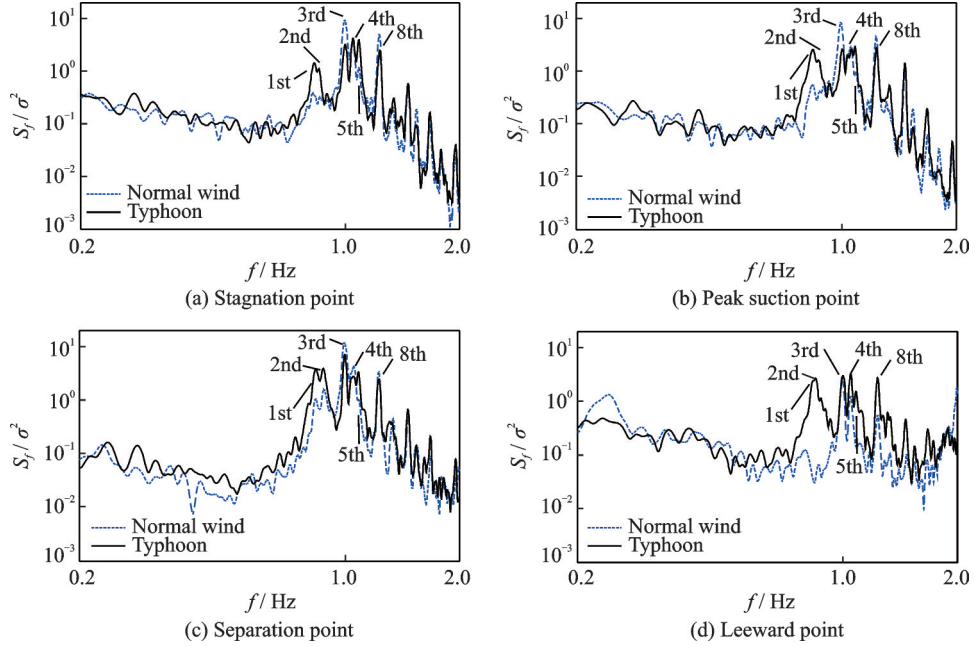


Fig.11 Displacement spectrum of structural response

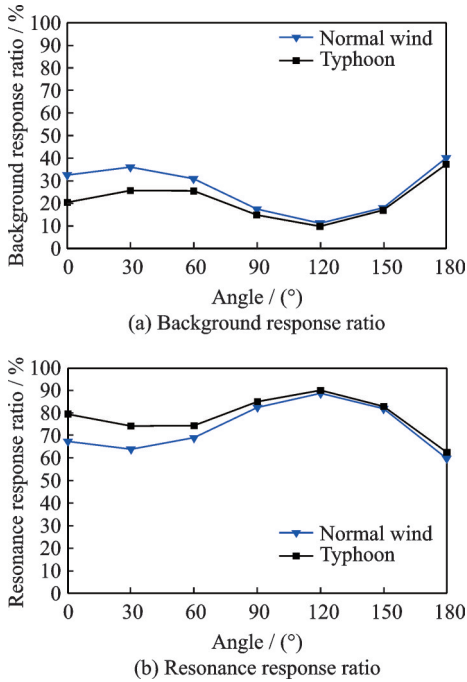


Fig.12 Background and resonance response ratio of total response under typhoon and normal wind

phoon are also analyzed. Except for the leeward point, wind-induced response generally obeys Gaussian distribution under normal wind. Non-Gaussian characteristic shows the separation point under typhoon condition.

3.2 Amplification effect

Structural response induced by stochastic fluctuation

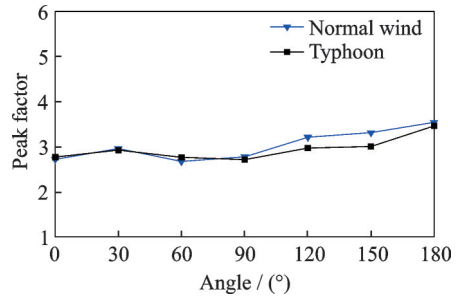


Fig.13 Peak factors of structural displacement response

Wind pressure is usually expressed by dynamic amplification coefficient β (Eq.(8)). The final design wind pressure can be quantified by Eq.(9) according to GLF method^[42]. Fig.15 shows the dynamic amplification coefficients under normal and typhoon. Dynamic amplification coefficient is up to the maximum value in the throat position in two kinds of environments, since resonance response ratio could reach the largest around circumferential angles (Fig.12(b)).

$$\beta = \frac{\bar{R} + g_p g \sigma}{\bar{R}} \tag{8}$$

$$\omega(z, q) = \beta C_p(q) F_1 \mu(z) \omega_{10} \tag{9}$$

where $\omega(z, q)$ is the design wind pressure, $C_p(\theta)$ the circumferential wind pressure coefficients every height, F_1 the interference coefficient, $\mu(z)$ the wind pressure profile, ω_{10} the wind speed of 10 m height, β the dynamic amplification coefficient, \bar{R}

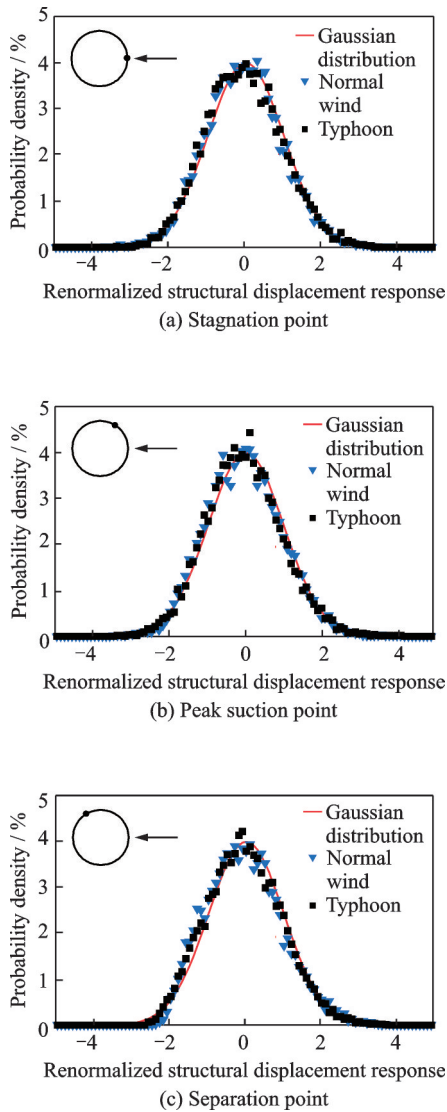


Fig.14 Probability density distributions of structural displacement response of three throat-region points under normal wind and typhoon

the mean response, g_p the peak factor, and σ the total fluctuation response. From normal wind to typhoon states, the dynamic amplification coefficient value gradually increases. The amplification coefficients of four key points at throat position are shown in Table 2. The maximum value is 1.80 under typhoon field and the maximum value is 1.52 under normal climate.

Table 2 Amplification coefficients of key points at throat position

Wind field	Stagnation point	Peak suction point	Separation point	Leeward point
Normal wind	1.10	1.12	1.52	1.50
Typhoon	1.22	1.27	1.80	1.61

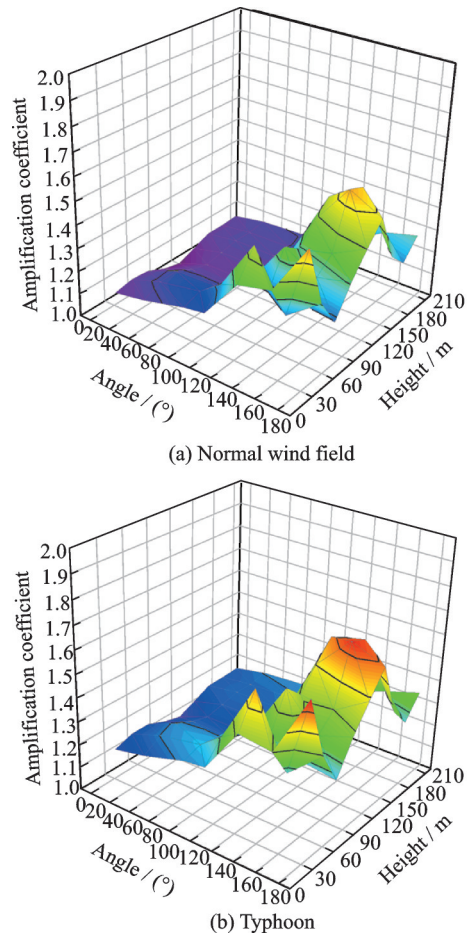


Fig.15 Dynamic amplification coefficients under normal wind and typhoon

4 Conclusions

Some conclusions from this investigation analyzing the wind pressure coefficients and structural response of a large cooling tower under normal wind and typhoon condition are reached as follows:

(1) Typhoon climate is be of stronger turbulence intensity and larger turbulence integral scale, up to 1.7 and 1.1 times than those under normal wind at the top of the cooling tower for a terrain Type B flow field. Moreover, the turbulence spectrum is lower from 0.01 Hz to 0.1 Hz and higher from 0.1 Hz to 1 Hz under typhoon.

(2) Model tests show that larger skewness and kurtosis for non-Gaussian wind pressure samples appear in the typhoon field, especially in the separation region. In accordance with the observation of non-Gaussian samples, the peak value of vortex component is higher under that of typhoon condition. It is indicated that free-stream turbulence af-

fects the vortex energy component of signature turbulence resulting in more organized vortex formation.

(3) Resonance response component of the cooling tower is the dominant of total response. The ratio of resonance response is bigger under typhoon condition and significant amplification effect on some structural resonance modes appears through analyzing renormalized structural response spectrum. It shows that the amplification effects in structural response level under typhoon climate are notable.

(4) The dynamic amplification coefficient on structural displacement level under typhoon field is up to 1.18 times than that under normal wind. The maximum value of dynamic amplification coefficient is shown at the throat position, which belongs to the adverse zone. It is necessary to adopt reasonable amplification coefficient to conduct wind-resistant designs of super-tall cooling towers under typhoon prone regions.

Reference

- [1] ARMITT J. Wind loading on cooling towers[J]. *Journal of the Structural Division*, 1980, 106: 623-641.
- [2] POPE R A. Structural deficiencies of natural draught cooling towers at UK power stations. Part 1: Failures at ferrybridge and fiddlers ferry[C]// *Proceedings of the Institution of Civil Engineers-Structures and Buildings*. [S.l.]: [s.n.], 1994: 1-10.
- [3] SOLLENBERGER N J, SCANLAN R H. Pressure-difference measurements across the shell of a full-scale natural draft cooling tower[C]//*Proceedings of the Symposium on Full-Scale Measurements of Wind Effects*. London, Ontario, Canada: University of Western Ontario, 1974.
- [4] NIEMANN H J, PRÖPPER H. Some properties of fluctuating wind pressures on a full-scale cooling tower[J]. *Journal of Wind Engineering & Industrial Aerodynamics*, 1975, 1: 349-359.
- [5] NIEMANN H J. Wind effects on cooling-tower shells[J]. *Journal of the Structural Division*, 1980, 106: 643-661.
- [6] SUN T F, GU Z F, ZHOU L M, et al. Full-scale measurement and wind-tunnel testing of wind loading on two neighboring cooling towers[J]. *Journal of Wind Engineering & Industrial Aerodynamics*, 1992, 43: 2213-2224.
- [7] SIMIU E, SCANLAN R H. *Wind effects on structures*[M]. New York: John Wiley & Sons, Inc., 1996.
- [8] ZHAO L, GE Y J, KAREEM A. Fluctuating wind pressure distribution around full-scale cooling towers[J]. *Journal of Wind Engineering & Industrial Aerodynamics*, 2017, 165: 34-45.
- [9] CHENG X X, KE S T, LI P F, et al. External extreme wind pressure distribution for the structural design of cooling towers[J]. *Engineering Structures*, 2019, 181: 336-353.
- [10] WINNEY P E. The modal properties of model and full scale cooling towers[J]. *Journal of Sound & Vibration*, 1978, 57: 131-148.
- [11] ZAHLTEN W. Time-domain simulation of the non-linear response of cooling tower shells subjected to stochastic wind loading[J]. *Engineering Structures*, 1998, 20: 881-889.
- [12] KE S T, GE Y J. The influence of self-excited forces on wind loads and wind effects for super-large cooling towers[J]. *Journal of Wind Engineering & Industrial Aerodynamics*, 2014, 132: 125-135.
- [13] ZHANG J F, GE Y J, ZHAO L, et al. Wind induced dynamic responses on hyperbolic cooling tower shells and the equivalent static wind load[J]. *Journal of Wind Engineering & Industrial Aerodynamics*, 2017, 169: 280-289.
- [14] ZHAO L, ZHAN Y Y, GE Y J. Wind-induced equivalent static interference criteria and its effects on cooling towers with complex arrangements[J]. *Engineering Structures*, 2018, 172: 141-153.
- [15] KE S T, WANG H, GE Y J. Comparison of stationary and non-stationary wind-induced responses of a super-large cooling tower based on field measurements[J]. *Thin-Walled Structures*, 2019, 137: 331-346.
- [16] YU M, ZHAO L, ZHAN Y Y, et al. Wind-resistant design and safety evaluation of cooling towers by reinforcement area criterion[J]. *Engineering Structures*, 2019, 193: 281-294.
- [17] GIAMMANCO I M, SCHROEDER J L, POWELL M D. GPS dropwindsonde and WSR-88D observations of tropical cyclone vertical wind profiles and their characteristics[J]. *Weather & Forecasting*, 2012, 28: 77.
- [18] HE Y C, CHAN P W, LI Q S. Observations of vertical wind profiles of tropical cyclones at coastal areas[J]. *Journal of Wind Engineering & Industrial Aerodynamics*, 2016, 152: 1-14.
- [19] KRAYER W R, MARSHALL R D. Gust factors ap-

- plied to hurricane winds[J]. *Bulletin of the American Meteorological Society*, 1992, 73: 613-618.
- [20] SHARMA R N, RICHARDS P J. A re-examination of the characteristics of tropical cyclone winds[J]. *Journal of Wind Engineering & Industrial Aerodynamics*, 1999, 83: 21-33.
- [21] ZHANG J W, LI Q S. Field measurements of wind pressures on a 600 m high skyscraper during a landfall typhoon and comparison with wind tunnel test[J]. *Journal of Wind Engineering & Industrial Aerodynamics*, 2018, 175: 391-407.
- [22] JEARY A P, FRIDLIN D, WANG L. Dynamic stability considerations for a natural-draft cooling tower under repair with hurricane-force wind action[C]// *Proceedings of 13th International Conference on Wind Engineering*. Netherlands, Amsterdam: [s.n.], 2011.
- [23] NISHI A, KIKUGAWA H, MATSUDA Y, et al. Active control of turbulence for an atmospheric boundary layer model in a wind tunnel[J]. *Journal of Wind Engineering & Industrial Aerodynamics*, 1999, 83: 409-419.
- [24] CAO S Y, NISHI A, KIKUGAWA H, et al. Reproduction of wind velocity history in a multiple fan wind tunnel[J]. *Journal of Wind Engineering & Industrial Aerodynamics*, 2002, 90: 1719-1729.
- [25] CAO S, TAMURA Y, KIKUCHI N, et al. Wind characteristics of a strong typhoon[J]. *Journal of Wind Engineering & Industrial Aerodynamics*, 2009, 97: 11-21.
- [26] GE Y, CAO S, JIN X. Comparison and harmonization of building wind loading codes among the Asia-Pacific Economies[J]. *Frontiers of Structural & Civil Engineering*, 2013, 7: 402-410.
- [27] National Standard Revision Group. GB50009—2015. Load code for design of building structures[S]. Beijing: Chinese Architecture & Building Press, 2015. (in Chinese)
- [28] MASTERS F J, VICKERY P J, BACON P. Standardized intensity estimates from surface wind speed observations[J]. *Bulletin of the American Meteorological Society*, 2010, 91: 1665-1681.
- [29] BALDERRAMA J A, MASTERS F J, GURLEY K R. Peak factor estimation in hurricane surface winds[J]. *Journal of Wind Engineering & Industrial Aerodynamics*, 2012, 102: 1-13.
- [30] KWON D K, KAREEM A. Comparative study of major international wind codes and standards for wind effects on tall buildings[J]. *Engineering Structures*, 2013, 51: 23-35.
- [31] Architectural Institute of Japan. AIJ—2004. Recommendations for loads on building[S]. Tokyo, Japan: Architectural Institute of Japan, 2004.
- [32] NISHI A, KIKUGAWA H, MATSUDA Y, et al. Turbulence control in multiple-fan wind tunnels[J]. *Journal of Wind Engineering & Industrial Aerodynamics*, 1997, 67/68: 861-872.
- [33] CAO S, NISHI A, HIRANO K, et al. An actively controlled wind tunnel and its application to the reproduction of the atmospheric boundary layer[J]. *Boundary-Layer Meteorology*, 2001, 101: 61-76.
- [34] TAMURA Y, SHIMADA K, HIBI K. Wind response of a tower (Typhoon observation at the Nagasaki Huis Ten Bosch Domtoren)[J]. *Journal of Wind Engineering & Industrial Aerodynamics*, 1993, 50: 309-318.
- [35] KOLMOGOROFF A. The local structure of turbulence in an incompressible viscous fluid for very large Reynolds numbers[J]. *Proceedings Mathematical & Physical Sciences*, 1991, 434: 9-13.
- [36] HARNACH R, NIEMANN H J. The influence of realistic mean wind loads on the static response and the design of high cooling towers[J]. *Engineering Structures*, 1980, 2: 27-34.
- [37] LAWSON T V. The use of roughness to produce high reynolds number flows around circular cylinders at lower reynolds numbers[J]. *Journal of Wind Engineering & Industrial Aerodynamics*, 1982, 10: 381-387.
- [38] ISYUMOV N, ABU-SITTA S H. Approaches to the design of hyperbolic cooling towers against the dynamic action of wind and earthquakes[J]. *Bull Int Assoc Shell Struct*, 1972, 48: 3-22.
- [39] ZHAO L, GE Y J. Wind loading characteristics of super-large cooling towers[J]. *Wind and Structures*, 2010, 3: 257-273.
- [40] SADEH W Z, SUTERA S P, MAEDER P F. Analysis of vorticity amplification in the flow approaching a two-dimensional stagnation point[J]. *Zeitschrift Für Angewandte Mathematik und Physik Zamp*, 1970, 21: 699-716.
- [41] SADEK F, SIMIU E. Peak non-Gaussian wind effects for database-assisted low-rise building design[J]. *Journal of Engineering Mechanics*, 2002, 128: 530-539.
- [42] DAVENPORT A G, ISYUMOV N. The dynamic and static action of wind on hyperbolic cooling towers: BLWT1-66[R]. London, Ontario, Canada: University of Western Ontario, 1966.

Acknowledgements The work was supported by the National Key Research and Development Program of China

(Nos. 2018YFC0809600, 2018YFC0809604) and the National Natural Science Foundation of China (No.51678451).

Authors Mr. XING Yuan will receive his Master degree in Tongji University, Shanghai, China, in 2020. His research interests include experiments and numerical studies on atmospheric boundary layer wind engineering and mainly focus on interference effect of group-structure.

Prof. ZHAO Lin received his Ph.D. from Tongji University, Shanghai, China, in 2003. He is currently a professor at Department of Bridge Engineering, Tongji University. His re-

search interests include bridge engineering and wind engineering.

Author contributions Mr. XING Yuan designed the study, compiled the models, conducted the analysis, interpreted the results and wrote the manuscript. Prof. ZHAO Lin, Dr. CHEN Xu, and Prof. GE Yaojun contributed to the discussion and background of the study.

Competing interests The authors declare no competing interests.

(Production Editor: ZHANG Huangqun)

台风环境下冷却塔风致振动的案例研究

邢源¹, 赵林^{1,2}, 陈旭¹, 葛耀君^{1,2}

(1. 同济大学土木工程防灾国家重点实验室, 上海 200092, 中国;

2. 桥梁结构抗风技术交通运输行业重点实验室, 上海 200092, 中国)

摘要: 冷却塔是风敏感结构, 其高度的增加使得抗风问题更加突出, 尤其是在台风地区。本文采用主动风洞技术模拟了场地为B类粗糙度的良态风和台风风场, 进行了某超大型冷却塔的刚性测压和气动弹性测振试验, 系统地研究了良态风和台风场下塔筒壳体抗风性能。对塔筒喉部位置迎风点、峰值吸力点、分离点和背风点处所对应壳体的风压系数、峰值因子、功率谱密度和动力放大系数进行综合研究。研究发现: 台风场下塔筒环向风压和风致响应存在更加明显的非高斯特征; 同时共振响应占比更高, 结构的动力放大因子最大值达到良态风作用下的1.18倍。本文的研究结果可作为台风地区超大型冷却塔抗风设计的参考。

关键词: 冷却塔; 主动风洞; 非高斯特征; 风致振动; 动力放大系数